NEUROIMAGE **6,** 93–103 (1997)
ARTICLE NO. NI970278

Parametric Analysis of fMRI Data Using Linear Systems Methods

Mark S. Cohen

UCLA Division of Brain Mapping, RNRC 3256, 710 Westwood Plaza, Los Angeles, California 90095

Received November 20, 1996

Using a model of the functional MRI (fMRI) impulse response based on published data, we have demonstrated that the form of the fMRI response to stimuli of freely varied timing can be modeled well by convolution of the impulse response with the behavioral stimulus. The amplitudes of the responses as a function of parametrically varied behavioral conditions are fitted well using a piecewise linear approximation. Use of the combined model, in conjunction with correlation analysis, results in an increase in sensitivity for the MRI study. This approach, based on the well-established methods of linear systems analysis, also allows a quantitative comparison of the response amplitudes across subjects to a broad range of behavioral conditions. Fit parameters, derived from the amplitude data, are relatively insensitive to a variety of MRI-related artifacts and yield results that are compared readily across subjects.

INTRODUCTION

Most of the data analysis approaches used in functional magnetic resonance imaging (fMRI) have their origin in the established methodology of positron emission tomography (PET) activation imaging. The two techniques differ in important ways, however, and it may be possible to achieve greater power (in the statistical sense) with fMRI by using analysis strategies that exploit its unique features. Both PET and fMRI take advantage of local changes in blood flow associated with increased or decreased neural activity (Belliveau *et al.*, 1991; Kwong *et al.*, 1992; Mazziotta and Phelps, 1984; Ogawa *et al.*, 1992; Roy and Sherrington, 1890). With $H_2\ ^{15}O$ PET, local increases in blood flow result in accumulation of radioactive tracer—typically collected over 30 s or so—the image intensity reflects the integral of the underlying neural activity. In fMRI, the images are acquired much more rapidly [using echo-planar imaging (Cohen and Weisskoff, 1991; Mansfield, 1977), acquisition times of less than 0.1 s are common] and the time course of the blood flow changes is revealed. In our original studies, we noted that the observed signal intensity change in MRI lagged the stimulus by several seconds (Kwong *et al.*, 1992). Optical imaging experiments have shown that blood flow changes display a multiphasic time course, presumably reflecting an initial oxygen depletion of the capillary bed, with a response latency of about 2 s, followed by a hyperoxygenation condition, in which increased blood flow exceeds local metabolic demand (Malonek and Grinvald, 1996). The significance of the excess oxygen delivery is not yet clear—it may reflect the need for delivery of other substrates, an anticipatory response for subsequent activations, a requirement for the clearance of metabolic byproducts, a failure of the vasculature to regulate blood flow precisely to the area of increased activity (Malonek and Grinvald, 1996) or, as Buxton has suggested recently (Buxton and Frank, 1997), it may be a consequence of the limited transit time of oxygenated blood through the capillary vasculature.

In addition to displaying a complex time course, the magnitude of the fMRI response does not bear an obvious simple relationship to either the underlying neural activity or the behavior (Boynton *et al.*, 1996). Even in the earliest reported studies, Kwong *et al.* (1992) noted that the MR signal increases were greater to visual stimulation at 8 Hz than to higher or lower rates. MR signal intensities are traditionally expressed in arbitrary units, as a plethora of factors affect the absolute signal intensity—tissue conductivity, coil placement, pulse sequence timing, tissue orientation, and magnetic field strength all play major roles. A consequence is that there exists no standard metric by which to describe the fMRI signal changes, making comparisons across studies difficult.

Our goal, in the present paper, is to address the problems of the fMRI time course and response magnitude by using a linear systems approach of a class similar to that reported recently by Boynton *et al.* and by Friston and colleagues (Boynton *et al.*, 1996; Friston *et al.*, 1994). We present data from the human visual and motor systems that suggest that this method will have useful applications in functional imaging. Our new method easily generalizes to the analysis of data sets collected with temporally irregular task periods and

1053-8119/97 $25.00

with parametric experimental designs (in the sense used by VanMeter *et al.* (1995)).

Typical fMRI Data Analysis Strategies

An important characteristic of functional imaging by magnetic resonance is that the signal changes are typically small (most experiments are presently performed at 1.5 T, where they are only a few percent) and occur in a background of substantial signal fluctuation that is not well correlated with the stimuli (Weisskoff *et al.*, 1993); contrast to noise ratios (CNRs) of 3 or 4 to 1 are typical, and a CNR of more than 8 is very unusual (and probably associated with large vessels). Thus, one of the key challenges in fMRI is the artifact-free detection of these small signal changes. One strategy, inherited from PET (Friston *et al.*, 1991), has been to look for changes in the mean signal intensity of the MR data during different behavioral conditions using Student's *t* test. Where no temporal information is available (as in traditional PET experiments) this is probably the best possible method, as the commonly used *t* test has unexcelled statistical power in detecting changes in mean (Press *et al.*, 1992). An alternative, though conceptually similar, analysis is to compare the intensity distributions in the behavioral conditions using the Kolmogorov-Smirnov (K-S) statistic. While not quite as powerful as the *t* test for detecting differences in mean, the K-S test can also be used to detect other differences in distribution, such as increased variance. It is a useful test when very little *a priori* information is available to differentiate the MR signal under different conditions. As many fMRI researchers have seen, however, type I errors are distressingly common in simple applications of the *t* or K-S statistic (see, e.g., Cohen *et al.*, 1996b). In response, some have advocated the use of "split-half" *t* test, which requires that the same pixel location exceed some predetermined *t* threshold on two independent acquisitions (Schneider *et al.*, 1993); the split-half test is very conservative and has been used as a way to improve detection rates for activation without introducing unacceptably high false positive rates (Constable *et al.*, 1995). Some have incorporated additional criteria, such as the number of contiguous locations of increased signal intensity (Schneider *et al.*, 1993; Worsley *et al.*, 1992), which impose somewhat arbitrary constraints on the minimum size of an "activated" brain region. An approach using multiple linear regression was recently outlined by Friston *et al.* (1995) that takes into account the time course of the fMRI signal in calculating *t* statistics.

An alternative method, pioneered by Bandettini, is to use correlation statistics to estimate the extent to which the signal in any pixel covaries with the behavioral conditions (Bandettini *et al.*, 1993). As the fMRI data are modeled poorly by differences in mean, especially when the task conditions are changing rapidly compared to the blood flow response, the correlation technique is frequently more appropriate than the *t* test. For slowly varying task conditions, the pixel intensity time course is usually cross-correlated with a boxcar function (square wave) and for more rapidly varying tasks a sinusoidal reference is commonly used (we note that for periodic tasks this is always a reasonable estimate, as it is the first component of the Fourier series describing the time course). Engel described the use of a periodic visual stimulus, whose position phase was linked to its spatial location (Engel *et al.*, 1994); he and others (Sereno *et al.*, 1995) have used similar stimuli to derive retinotopic maps of the human visual cortex. The method described below also exploits the correlation approach.

Linear Systems Analysis

The well-developed tools of linear systems analysis (see, for example, Liu and Liu, 1974) used widely in electrical and mechanical engineering can be used to predict the responses of certain systems to a wide variety of inputs. In particular, for a true linear and time-invariant (LTI) system, the response to an arbitrary input is equal to the convolution of that input with the system's so-called impulse response or transfer function. From the outset, we note that no physical system actually obeys these constraints. On the other hand, the technique gains its tremendous power from the realization that many systems closely approximate LTI behavior over a useful range of boundary conditions. Our goal in the present work has been to develop an LTI model of the observed fMRI signal response. This modeled response is then correlated with the signal intensity time course in each voxel in the MR image series to detect active regions.

To the extent that the transfer function of the fMRI signal is modeled properly, it is possible to anticipate the response to more complex stimuli. It has been shown, for example, that the magnitude of the observed MR signal has a highly nonlinear response to variations in stimulus characteristics, such as the rate of a blinking light stimulus (Kwong *et al.*, 1992), the intensity contrast of a visual stimulus (Tootell *et al.*, 1995), or the rate of hand motion (Bookheimer *et al.*, 1995; Cohen *et al.*, 1995; Dobkin *et al.*, 1996; VanMeter *et al.*, 1995). We proposed that the response profiles of different brain regions to parametric variations in stimulus characteristics form a powerful tool for understanding and detecting component processing of complex stimuli and behaviors (Cohen *et al.*, 1995) that is more amenable to physiologic interpretation than is a *t* statistic, a probability level, or a correlation coefficient. Here, we show that with a reasonable estimate of the brain impulse response, we can perform parametric analyses

that respect the temporal characteristics of the brain blood flow response.

METHODS

Response Models

For the present experiments, the brain impulse response was estimated based on data collected by R. L. Savoy and colleagues (Savoy *et al.*, 1994). Summarized briefly, they presented visual flash stimuli of various durations and averaged the fMRI signal time course in visual cortex to repeated stimulation in order to assess the sensitivity of fMRI recordings to very short duration stimuli; their experiments used flashes of 34 ms, 100 ms, or 1 s. We fitted the data from the averaged responses to 1-s stimuli to a three-parameter gamma variate function using the Levenberg-Marquardt algorithm, as shown in Fig. 1. In these experiments, we use the parameter values

$$\mathrm{SI}(t) = kt^{8.60}e^{-t/0.547}, \tag{1}$$

where k is adjusted to give unit amplitude at equilibrium, i.e., when stimuli are repeated often enough for the estimated response to reach a constant peak. To form estimates of the blood flow response to arbitrary task inputs, we form the convolution of the task with this blood flow response. This is shown for a simple Off–On–Off–On–Off task in Fig. 2. The typical lag in the vascular-based MR response is clearly visible in the estimated response, suggesting visually that this impulse response estimate is reasonable. A chief advantage of our method, however, will be its ability to estimate the responses to more complex behavioral conditions.

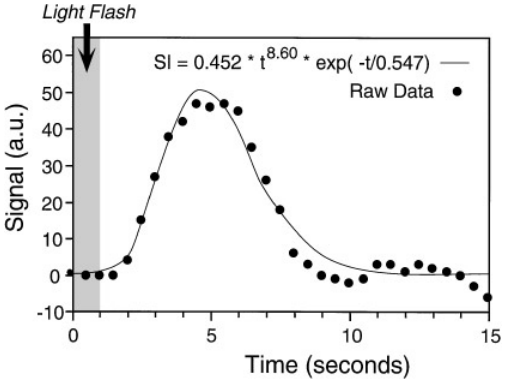

FIG. 1. Averaged fMRI response (·) to 10 repetitions of a 1-s light flash stimulus as measured in the visual cortex of a volunteer (data from R. Savoy). Shown in a thin line is the fitted response using a gamma variate model (Levenberg-Marquardt algorithm).

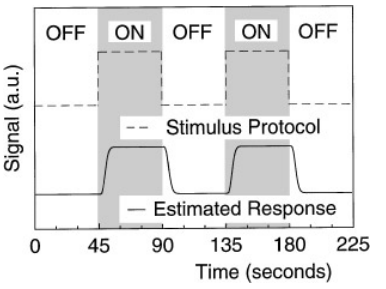

FIG. 2. Estimated fMRI response to visual stimulation consisting of alternating 45-s rest and stimulus periods. The gray bars indicate stimulus periods and the estimated response is formed by convolving the stimulus time course (dashed lines) with the impulse function of Fig. 1.

MR Imaging

Subjects

All subjects for this study were normal volunteers between 25 and 40 years of age without neurological abnormalities. All experiments were performed under informed consent and guidelines approved by the UCLA Human Subjects Protection Committee.

Imaging

We performed our scanning on a 3-T magnetic resonance imaging system (General Electric, Waukesha, WI) designed specially for applications in functional MRI (Cohen *et al.*, 1996a). Prior to any anatomical imaging, we shimmed the magnet for linear and quadratic terms using an image-based "quickshim" procedure provided by the manufacturer and modified by us to give corrected values. After shimming, the field homogeneity over the entire brain was typically better than 50 Hz (<0.5 ppm). We then acquired localizer images using conventional sagittal fast SPGR imaging (TR = 13.9, TE = 2.8 ms, Flip = 20°, TI = 700, 32 slices, 5 mm 3D, 256 × 256 matrix). A series of 4-mm axial echo-planar images (EPI) (Advanced NMR Systems, Wilmington, MA) was then taken with 1-mm gaps to span the range from the superior pole to the base of the cerebrum. Our EPI scans are performed with a sinusoidal readout gradient oscillating at 1.4 kHz to minimize shape distortions (Farzaneh *et al.*, 1990). This frequency and resolution together necessitate gradient strengths of approximately 3.6 G/cm. For these T2-weighted images, the matrix size was 128 × 128, FOV = 20 cm (pixel size 1.5 × 1.5 mm), half-Fourier acquisition (Cohen and Weisskoff, 1991; Margosian, 1985), TR = ∞. From the axial slices, we identified one to three slices, on the basis of sulcal anatomy, that contained the hand sensorimotor area anterior and posterior to the central sulcus; these were used for the subsequent functional imaging studies. For the visual system experiment, we identified the calcarine fissure from sagittal slices and

prescribed graphically a series of slice orthogonal to the line that best fit this sulcus.

We acquired functional images with BOLD contrast weighting by using a gradient echo imaging sequence with an echo time of 45 ms, equal to the measured T2* of the brain on our system. For the motor experiments, we used a TR of 2 s and a flip angle of 80°; for the visual tasks we used a TR of 2.5 s. The measured T1 of the brain gray matter in our system brain is approximately 1200 ms; our imaging parameters were thus optimized for maximal signal intensity at the expense of some blood inflow-dependent contrast. These images were acquired with a matrix size of 64 × 128 over the 20-cm FOV, resulting in an in-plane resolution of approximately 1.5 mm × 3 mm.

Behavioral Protocols

Visual system task. Subjects were presented a flashing checkerboard pattern, with black and white features switching at approximately 8 Hz. The visual stimulus was generated on an Apple Macintosh computer system (Apple Computer, Cupertino, CA) and was presented binocularly on a magnet compatible LCD television system (Resonance Technology, Van Nuys, CA). Stimuli subtended approximately 15° of visual angle. Subjects were instructed to look at a fixation point present during the stimulation. During rest periods, the screen was switched to a neutral gray with the same mean luminance as the checkerboard stimulus.

Motor tasks. To test our model for complex timing, we used a finger opposition task in which the subject was instructed to alternately oppose each finger to the thumb in a complex repeating order (i.e., 1-3-2-4-4-3-2-1 . . .) in brief (10 s), irregular intervals as described in the legend to Fig. 4A. Based on our models, we expected that this would result in fMRI signal changes 90° out of phase with the behavior (Fig. 4A). The timing was designed also as an example of a protocol not readily analyzable using sinusoidal models.

For the motor rate experiments, the subjects listened to a click stimulus, generated by a metronome, at three different rates of 52, 104, and 208 beats/min (0.867, 1.73, and 3.47 Hz) delivered binaurally through MRI compatible headphones (Resonance Technology). The subjects performed the finger opposition task, as described above, in time with the click stimulus, using the dominant hand. Periods of finger motion were alternated with periods of rest, and the rate order was counterbalanced across subjects, or, where time allowed in one subject, across trials (Fig. 5). The auditory stimulus remained on during the rest periods, and the rate changes occurred halfway through the rest blocks. The subjects were given brief verbal instructions ("Move now"; "Rest now.") to indicate when they should start or stop the hand motions. All subjects were tested for their ability to perform the motor task at the given rates and were interviewed following the scan to determine if they experienced any difficulty. None did.

Data Analysis

Our data analysis approach was designed to compare and contrast analysis strategies. In all cases the images were first thresholded using a histogram normalization procedure so that only pixels within the head were evaluated. Our algorithm detects the most frequently occurring value within the bottom 15% of the signal range and sets the threshold to three times this value. The statistical tests were given signed values to indicate regions which were correlated or anticorrelated with the behavioral tasks. In the experiments reported here, only positive changes were appreciable. The final statistical maps were thresholded, as indicated below, and superimposed on the coplanar EPI images acquired immediately prior to the functional studies. For the data comparing response amplitudes across subjects (Table 1), the images were subjected to a 3 × 3 in-plane Hanning filter to minimize noise prior to statistical analysis.

Student's t test. Images acquired during periods of stimulation were pooled and compared pixel-by-pixel with periods of rest using Student's *t* test corrected for unequal variance. To account for the characteristic lag between stimulus and fMRI response, we also calculated the *t* statistic with time shifts of 2 to 8 s. In our studies, a lag of 6 s resulted in the maximum *t* values.

Correlation maps and intensity estimates. We constructed the correlation maps in several steps. First, we identified the motor cortex anatomically on the basis of

TABLE 1

Comparison of Statistical Results Using Student's *t* Test or the Pearson Correlation Coefficient to Detect Activation of Hand Motor Cortex from the MRI Time Intensity Curves

Reference method	Raw statistic	Equivalent *t*
t statistic		7.57
Time-shifted (6 s) *t* statistic		21.99
Correlation with square function	0.5717	10.34
Correlation with shifted square function	0.8959	66.64
Correlation with sine function	0.7707	26.04
Correlation with shifted sine function	0.9086	76.96
Correlation with linear estimate	0.9337	109.05
Correlation with weighted linear estimate	0.9645	210.69

Note. As the MRI response clearly lags the stimulus, the tests were also compared with the behavioral input shifted by 6 s to maximize the statistics. The final row in the table shows the correlation coefficient calculated between the actual MR data and the response estimate of Fig. 6. To compare the results of the *t* and correlation statistics, the last column shows the probability of type 1 error with these data.

sulcal anatomy, as described above, and then on the basis of functional anatomy. For the latter, we determined the correlation coefficient between the response estimate, computed as described above, for only the highest stimulus rate (which yielded the strongest response) and the pixel-wise signal intensities in the functional image series. Pixels whose signal intensity changes had a correlation coefficient of 0.5 or greater with the stimulus were then selected.

The signal intensity changes were computed as the slope of the linear fit of the MR signal intensity to the estimated response. By using this algorithm, the measured intensity changes are matched to the temporal characteristics of the fMRI response. The slope was computed on a pixel-by-pixel basis and expressed as the percentage signal change at the selected stimulus rate (e.g., Fig. 7).

The overall time course was fitted to the response estimates by determining the slope, as above, for each stimulus rate individually. The response estimate overall was formed by convolving the amplitude-weighted description of the behavioral task with the impulse response shown above, weighted by the response magnitude at each stimulus rate. This response estimate is therefore a description of the response pattern of primary motor cortex to parametrically varied input.[1]

RESULTS

Signal Intensity Time Course

As reported in many publications using similar protocols (e.g., Kwong *et al.*, 1992), periods of visual stimulation were followed at a latency of a few seconds by increased signal intensities in the visual areas of the brain, including the calcarine cortex, or V1. After cessation of the visual stimulation, the signal did not return immediately to baseline, but instead decreased gradually over approximately 15 s. The estimated response, based on the convolution method, and the corresponding measured data are shown in Fig. 3.

Since the impulse response form was determined within the visual system, albeit from another scanner at a lower field strength, on a different subject, and using slightly different imaging procedures, we were gratified to see that the response estimate approximated many features of the measured data, including the delayed rise to peak response and the slow decay to baseline signal. Note that the signal increase is large (approximately 30%) at this field strength as predicted by Fisel, Turner, and others (Fisel *et al.*, 1991; Turner *et al.*, 1993).

The results of the motor timing task, shown in Fig. 4A, also demonstrated that the response form was

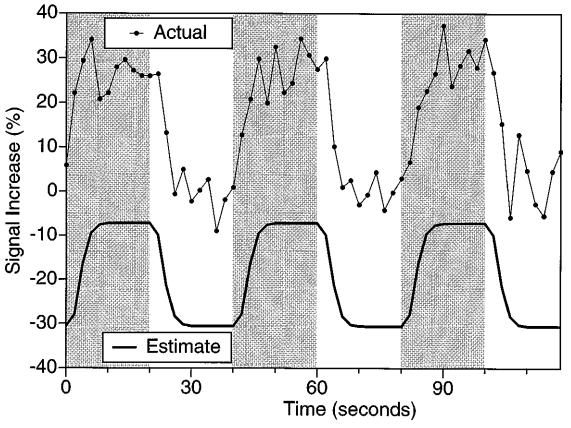

FIG. 3. *A priori* response estimate for the flashing checkerboard visual stimulation protocol. (Top) Measured signal intensity time course in calcarine cortex. Gray bars indicate periods of visual stimulation.

estimated well using the convolution procedure, even though the impulse response was derived from an entirely different neural system. In this case, because of the rapid left–right hand alternation, the measured responses were shown clearly to lag the behavior by 90°. A *t* map of the differences in mean during periods left and right hand movement (Fig. 4B) shows no focal in right motor cortex and artifactually elevated signal in left motor cortex (due to the phase shift). The correlation map with the estimated response (Fig. 4C) demonstrates clearly several areas of activity near the central sulcus (presumably primary motor and sensory areas) and in the midline (representing supplementary motor areas). Figure 4D is considered in more detail below. Clearly, the timing for the task in Fig. 4 was designed as a worst case scenario for a naive analysis using the *t* statistic in fMRI. It does, however, illustrate just how badly the interpretation of the MRI data can be distorted if the signal time course is not respected. In Table 1, we show how the addition of a phase lag can mitigate, but not eliminate, this problem.

We used the linear fitting procedure outlined above to provide a quantitative estimate of the response magnitude at each hand motion frequency. These intensity weightings were applied to the impulse response function of Fig. 1 to come up with the estimated response profile shown in Fig. 5, which shows the signal intensity time course, the amplitude-weighted fit to the time course estimate, and the error term, created by subtracting the actual data from the fitted response. The responses were clearly nonlinear in amplitude as a function of finger tapping rate [as noted previously (Cohen, 1996; Cohen *et al.*, 1995)]. The error term was uncorrelated with the stimulus ($R^2 \ll 0.01$), suggesting that the model explained most of the stimulus correlated signal. Figure 5 shows the locations of pixels with correlation coefficients greater than 0.3 or less than

[1] The software tools used to perform this data analysis are freely available for non-commercial academic use at our world-wide web site: http://brainmapping.loni.ucla.edu.

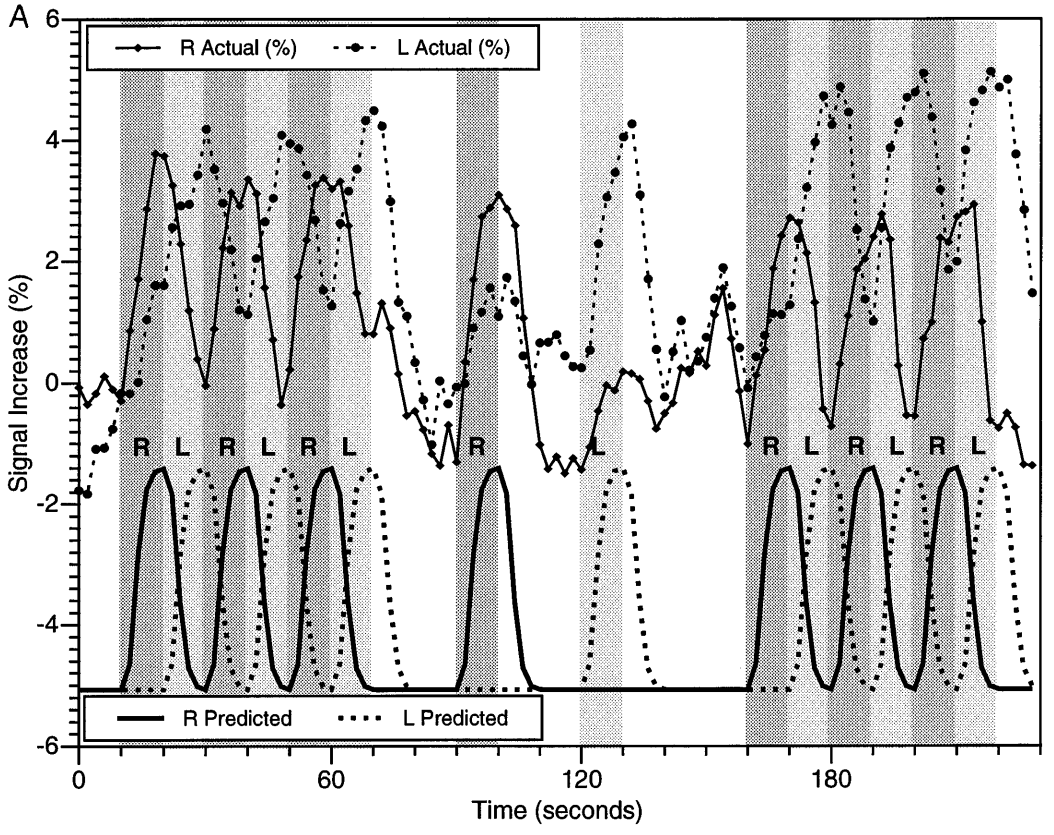

FIG. 4. (A) Time course of motor timing experiment and the estimated and actual fMRI responses. Dark and light gray bars represent periods of right- and left-hand motion, respectively, as indicated also by the letters R and L. During these periods the subject was instructed to repeatedly oppose her fingers to her thumb as rapidly as possible in the order 1-2-3-4-4-3-2-1 using the indicated hand. The hands were used in alternation for 10-s intervals, in some cases with intervening rest intervals. The behavioral time course for the left and right hands were convolved, individually, with the impulse response of Fig. 1, resulting in the estimated responses shown by the heavy solid and dashed curves, for right and left hands, respectively, as shown on the graph at bottom. These curves are seen to lag the behavior by about 90°. The measured fMRI time course is shown in lighter solid and dashed lines at the top of the graph for the corresponding (contralateral) primary motor and sensory areas. The signal amplitudes are compared to the mean signal at rest. (B) Map of t statistic comparing periods of left- and right-hand motion. Because of the phase lag between hand motion and activation, the simple t map fails to show regions of strong focal activation. (C) Map of pixels showing a correlation of 0.5 or greater between the MR signal intensity and the estimated responses from A. Obvious focal areas are evident in the cortex contralateral to the hand motion. Some midline structures also show hand-specific activity. (D) Estimated response amplitude (see below) for pixels detected in C.

−0.3 (anti-correlated) and their estimated response magnitudes. Figure 9 compares the response to three different tapping rates for two additional subjects.

Figure 7 demonstrates the linear fitting results. The data are "rotated" such that the fMRI signal is plotted as a function of the response estimate. The slope of that fit is used for magnitude estimation. In this case, a signal increase of 10.2% is associated with a rate of 208 taps/min. Note that the linear fit is a good estimator to the transformed data, showing an R^2 of 0.930.

Figure 8 shows a map of the correlation coefficient and of the slope of the signal change (from the same data set as in Fig. 5) as determined by this fitting procedure. Comparing the two maps, it is obvious that they provide different but complementary information. The regions showing the greatest signal change may not be the best correlated with the stimulus and vice versa.

Comparison of Statistical Results

As a measure of the relative performance of our linear estimation procedure, for the same 31-pixel ROI we compared the t statistic and correlation with square functions and sinusoids, with and without a time shift, to the impulse convolution approach, with amplitude weightings determined by measurement of the signal change. These results are shown in Table 1 and are presented as equivalent t statistics (Press *et al.*, 1992).[2] Formally, the correlation with the weighted linear estimate is of dubious statistical value, as the template

[2] The correlation coefficient can be converted conservatively to a t distribution according to the formula

$$t = cc\sqrt{\frac{(N-2)}{((1-cc)^2)}}.$$

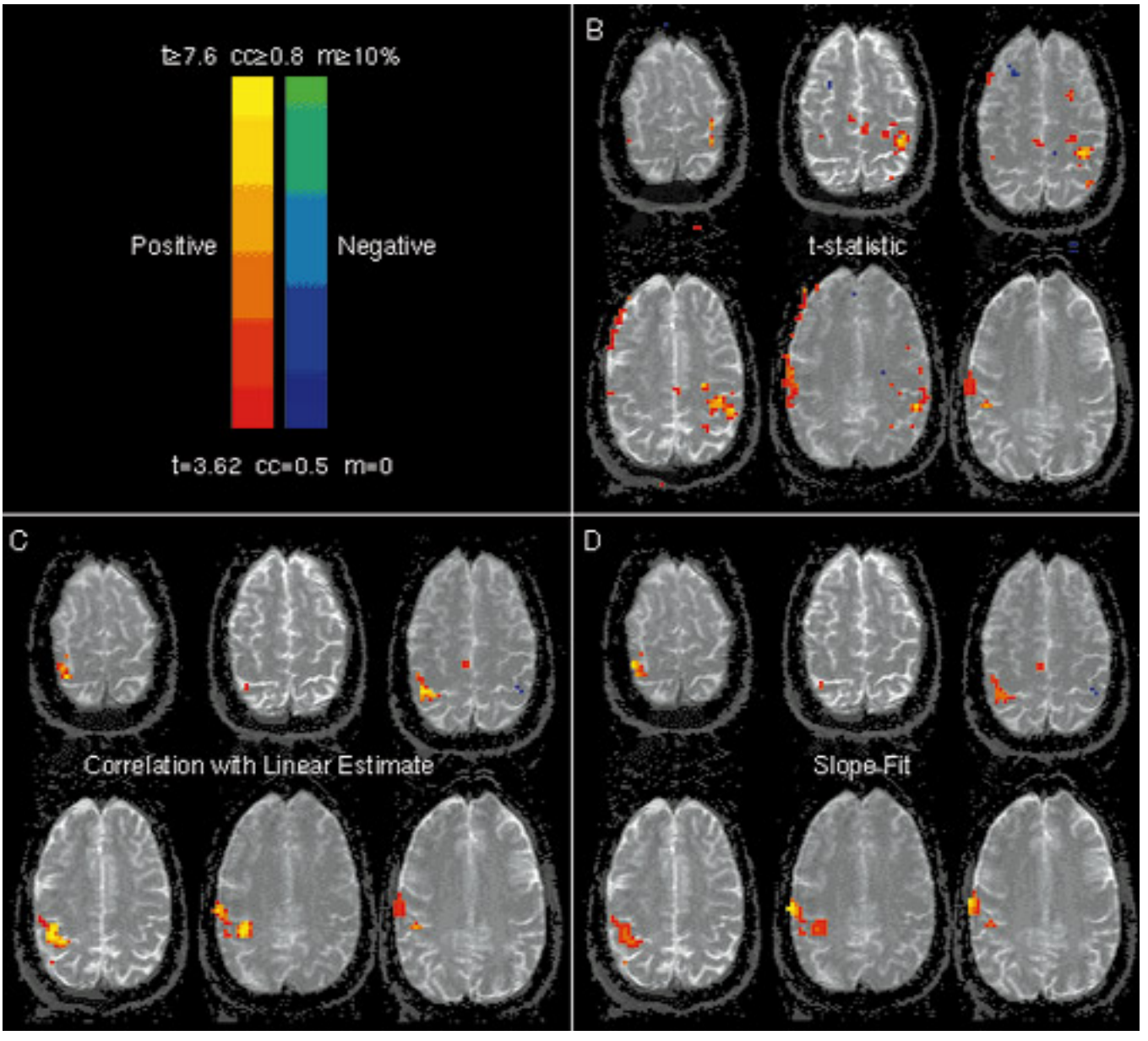

FIG. 4.—Continued.

was formed based on the data. We present the correlation as evidence of the completeness of the fit. Although we eschew the use of probability estimators in fMRI in many cases (Cohen *et al.*, 1996b), the data collected suggest a probability of type I error, using this method, of much less than 1×10^{-99}.

Parametric Characterization of fMRI Response

The slope-fitting procedure outlined above allows us to estimate the magnitude of the fMRI response to different stimulus conditions. The signal intensity increases calculated from the maximum finger tapping rate ranged from 6 to 10.2% in our subjects. Based on prior work (Cohen *et al.*, 1995) we anticipated a logarithmic signal intensity (SI) response to the stimulus of the form

$$\mathrm{SI} = A(1 - e^{-r/B}), \tag{2}$$

where A is a fit constant describing the amplitude and B describes the relationship among finger tapping rate, r, and signal change. Normalizing the data from three subjects to the signal change at the maximum, by setting $A = 1$ we used the Levenberg-Marquardt procedure to estimate B for all subjects. In these experiments B ranged from 44.2 to 75.3, showing reasonable unifor-

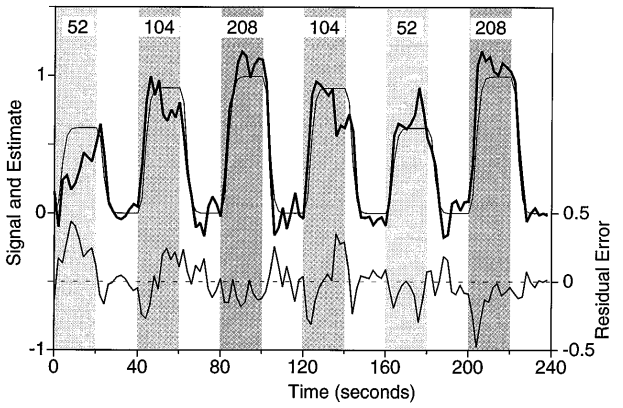

FIG. 5. Heavy lines show the fMRI signal intensity as a function of finger tapping rate. The light lines show the time intensity behavior predicted using the LTI approach. At bottom is the residual error—simply the difference of the two curves at top. The finger tapping rate, in counts per minute, is shown by the numbers at the top. Gray regions indicate periods of hand motion.

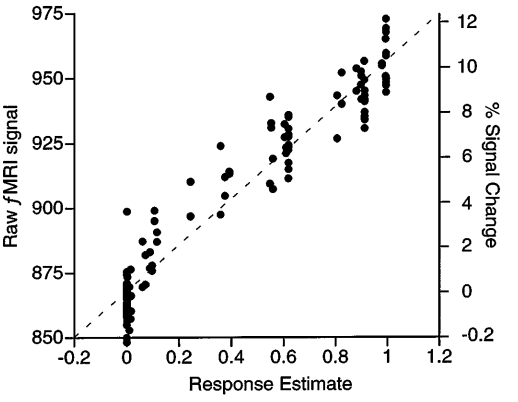

FIG. 7. Actual fMRI signal strength plotted as a function of the estimated response obtained by the convolution and fitting procedure, from the same subject shown in Fig. 6. Line indicates the best linear fit. The slope of this line can be used as an estimate of the response intensity.

mity across subjects of the response form. These data are shown in Fig. 9. We note that the response magnitude, *A*, is a less effective comparison, as it may depend on factors such as the RF flip angle in that region of the brain, the size, shape, and orientation of blood vessels, and a wide variety of other factors.

DISCUSSION

In this paper, we have developed a model for the temporal behavior of fMRI signals that is based on the theory of linear systems. We have then extended these results to a procedure for amplitude fitting that is piecewise linear. Together these results may be applied to the analysis of relatively complex behavioral conditions with irregular timing and variable intensities. While many behavioral and sensory conditions may be evaluated with stereotyped periodic timing, this still represents a practical limitation on fMRI protocols. For example, the data shown in Fig. 4 suggest that in certain behaviorally reasonable protocols the time lag between activity and response can lead to an apparent 180° phase shift in signal. In that example, left hand motor activity appeared using simple *t* statistics to be linked to left motor cortex signal changes. Using our fitting procedure, it is possible to predict brain responses to irregularly timed stimuli (an advantage of the *t* statistic as well), while respecting the intrinsic fMRI time course.

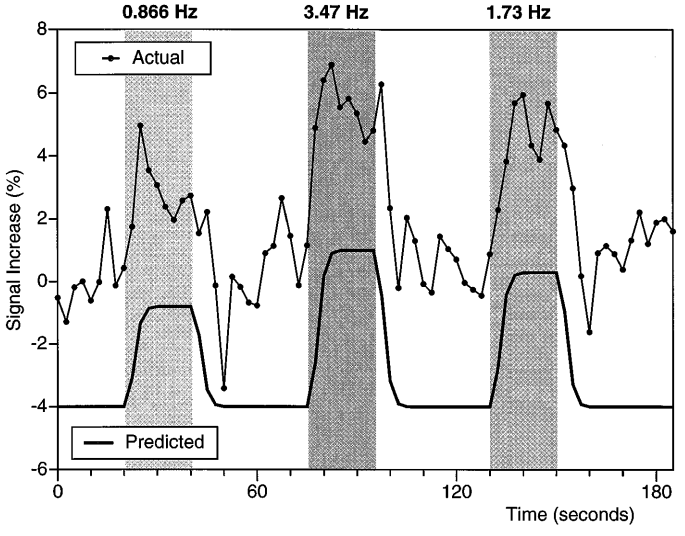

FIG. 6. (Left and right) fMRI signal intensity as a function of finger tapping rate. Heavy lines show the time intensity behavior predicted using the LTI approach, lighter lines and points show the actual data from two different subjects.

Behavioral protocols of interest in functional imaging may be variable in intensity as well as in rate, and the relationship between stimulus characteristics and the magnitude of signal change can help to differentiate functionally distinct brain regions. The small and relatively homogeneous residual errors after amplitude-weighted curve response prediction (Fig. 5) demonstrate that the convolution approach can help to extract intensity patterns of fMRI signal changes. Although absolute signal intensity is not a reliable measure in fMRI, the parametric signal response can be readily normalized, as in Fig. 5; after this transformation, they are relatively stable across subjects, as suggested in the data of Figs. 6 and 9. A typical procedure might be to fit the fMRI response to a known locus of activation and to use the fitted function as a template to explore other regions of cortex in the same or different subjects that might behave similarly or differently.

Compared to either simple application of the *t* statistic or to correlation with less accurate reference functions such as square or sine waves, the convolution

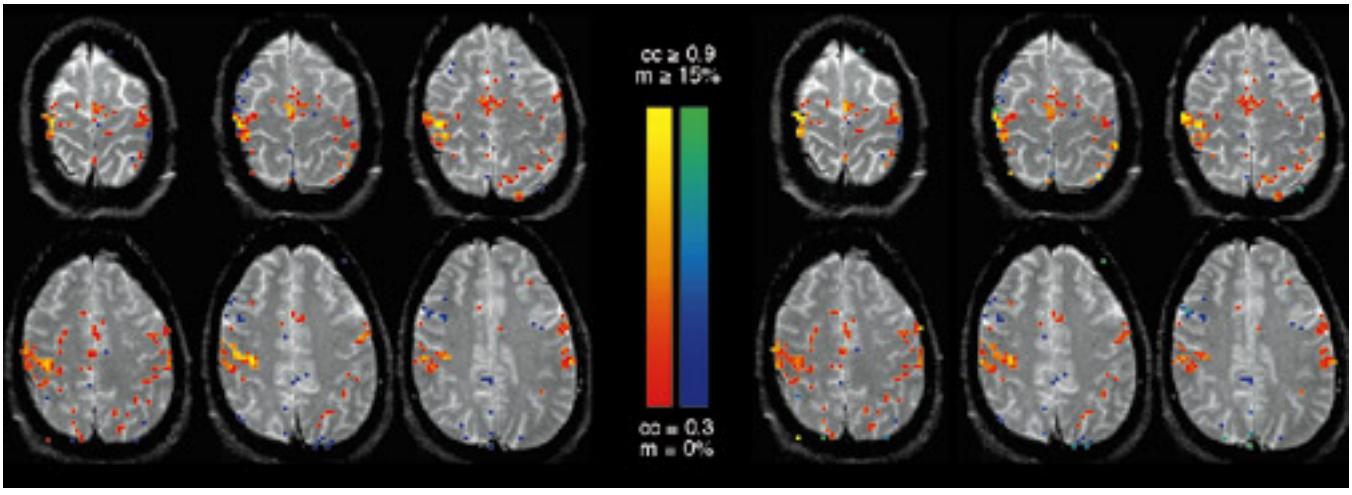

FIG. 8. Map of activation for the same subject, with color intensity representing the value of the correlation coefficient (left) and slope fit (right), as indicated by the color bars in the center. Positive values are indicated in colors from red to yellow; negative values range from blue to green.

approach offers gains in both sensitivity and specificity. The dramatic increases in the *t* statistic, shown in Table 1, attest to this fact. Although correlation with a time-shifted sine function is almost as powerful in this case, out method allows fitting to data of arbitrary timing (e.g., Fig. 4) that could not be fitted to sinusoids.

Friston *et al.* (1994) showed that the observed fMRI response could be estimated by convolution of the behavioral timing with a Poisson function describing the autocorrelation of the fMRI signal. This approach has the advantage that it can be derived from the actual data set. Further, the form of the function used is grossly similar to the impulse response used in this report. The Friston method also has the advantage that it would be possible to determine a separate autocorrelation function for each voxel in the imaging volume and thus to account for spatial variations in this parameter, though that is not proposed in their work. It is not safe to assume, however, that the impulse response is a Poisson function, and we felt that it was better to use the more directly measured response function. Boynton and colleagues (Boynton *et al.*, 1996) have demonstrated some of the boundary conditions of the linear approximation for fitting of the time curves. Indeed, our own data (Fig. 5) suggest limitations to the accuracy of the temporal fit. For example, in several of the on–off periods, the model timing appeared to be slightly slower than the actual response, resulting in an error term that was significant during rising and falling phases of the time intensity time course. More than likely, this results from using an impulse response derived from the visual cortex to model motor activity in parietal areas, where the hemodynamic delays may differ. Clearly, the technique will become more powerful as better impulse response estimates become available for different cortical regions. One approach to deriving these might be mathematical deconvolution of the fMRI time course and behavior—an area that we are exploring currently. Although the tests included here are by no means comprehensive, they indicate a range of conditions in which the methods of linear systems analysis may be used to predict the fMRI responses. Our own work, for example, involves the detection of signal changes associated with spontaneously occurring hallucinations (Cohen and Green, 1995) or epileptic seizures (Bookheimer, 1996; Bookheimer and Cohen, in press) as in the studies reported by Warach and Jackson (Jackson *et al.*, 1994; Warach *et al.*, 1994). In these cases the analysis procedure cannot depend on the presence of periods of fixed duration or rate. Our procedure places no such constraints on the experimental design and may be used in studies without prior knowledge of the behavioral or stimulus time course. Because the impulse response is causal (affecting the signals only for images which follow the stimulus), it

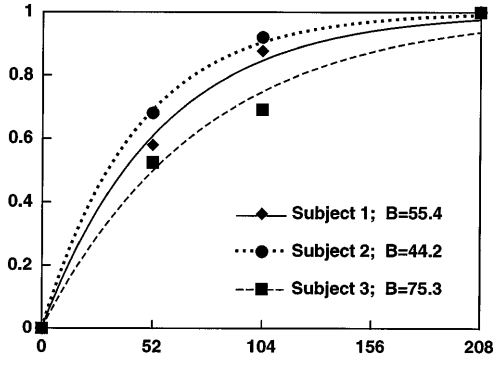

FIG. 9. Normalized response amplitudes for three subjects as a function of finger tapping rates. Lines represent best fit to a function of the form: $SI = (1 - \exp(-r/B))$, where r is the tapping rate. The fitted values of B are indicated for each subject.

may be implemented in a real-time analysis system, as is the goal of our laboratory (Hong, *et al.*, 1997). Recent work by Menon at very high magnetic field strength has suggested that the initial hypo-oxygenation phase may be seen with MRI (Menon *et al.*, 1995). As we have not yet replicated this finding in our own experiments, this behavior has not been included in the models developed here, though it may be incorporated readily.

MRI activation imaging has suffered from the limitation that the statistical analyses used to indicate the presence or absence of activation responses involve numerical transformations of the data that tend to distort the apparent activation magnitude, since the statistical confidence is scaled inversely with the local uncorrelated signal fluctuation at each location. This limitation is confounded further in PET studies that frequently require the pooling of data from several subjects. In this case, the statistical detectability of a regional activation is also modulated by the intersubject variability of the individual's structural or functional anatomy. The slope and correlation maps (e.g., Figs. 4 and 8) show different information. A simple explanation might be that the areas of large signal change represent veins draining a relatively large territory. While their high blood concentration results in relatively large signal change, their pulsatility reduces their correlation with the stimulus. Alternatively, it may be that our impulse response is for some reason a poor model of the fMRI response in those regions. The latter possibility is particularly important for parametric study designs. Neither our model nor other models of which we are aware account fully for regional differences in cerebrovascular coupling or nonstationary autocorrelation structures, and both of these may be important factors influencing the form of the fMRI response. The piecewise linear approach that we have adopted to approximating the parametric form of the response is not the only, or even necessarily the best, choice. In their 1995 paper, Friston *et al.* described the use of multiple linear regression perform equivalent fits. The two approaches are computationally similar, and either can be used to describe the functional form of the fMRI signal response.

We believe that an important use of the parametric analysis method developed here will be its ability to differentiate the activation of various brain regions on the basis of details of their response profiles. In a PET study, for example, Price *et al.* (1992) showed that the rCBF in primary auditory cortex was correlated with the rate of word presentation, whereas the rCBF in superior temporal gyrus was not, though both areas showed increased rCBF with words as opposed to rest. Grasby *et al.* used a parametric analysis to study the relationship between PET-derived rCBF and word list length. In a PET study of the activation magnitude as a function of finger tapping rate, Blinkenberg and coworkers reported that the slope of the response as a function of tapping rate distinguished among cortical areas (Simpson *et al.*, 1995). A paper by VanMeter and colleagues uses parametric analyses to characterize the activation of a variety of motor and premotor regions as a function of the rate of a motor task. Recently, Büchel and colleagues (Büchel *et al.*, 1996) developed a nonlinear regression approach, based on the general linear model, which promises to yield results analogous to ours in PET imaging, albeit without the ability to fit the signal time course. In studies of the effects of stimulus presentation rate in the auditory cortex, Binder and colleagues reported response profiles qualitatively similar to those we show here in the motor system (Schroeder *et al.*, 1995). While with suitable assumptions and normalization, it is reasonable to discuss PET experiments in terms of cerebral blood flow, functional MRI using the BOLD mechanism does not lend itself readily to this sort of quantitation. We believe that our methods act to overcome this limitation and thereby allow the direct comparisons of activation magnitudes across subjects.

REFERENCES

Bandettini, P. A., Jesmanowicz, A., Wong, E. C., and Hyde, J. S. 1993. Processing strategies for time-course data sets in functional MRI of the human brain. *Magn. Reson. Med.* **30:**161–173.

Belliveau, J. W., Kennedy, D. N., Jr., McKinstry, R. C., Buchbinder, B. R., Weisskoff, R. M., Cohen, M. S., *et al.* 1991. Functional mapping of the human visual cortex by magnetic resonance imaging. *Science* **254:**716– 719.

Bookheimer, S. 1996. Functional MRI applications in clinical epilepsy. *Neuroimage* **4:**S139–S146.

Bookheimer, S., and Cohen, M. 1997. Functional MRI. In *Epilepsy, A Comprehensive Textbook* (J. Engel and T. Pedley, Eds.). Raven Press, New York. [in press]

Bookheimer, S. Y., Cohen, M. S., Dapretto, M., Fried, I., Shewmon, A., Black, K., *et al.* 1995. Functional MRI in surgical planning. In *Society for Neuroscience*, Vol. 21, p. 273. San Diego, CA.

Boynton, G. M., Engel, S. A., Glover, G. H., and Heeger, D. J. 1996. Linear systems analysis of functional magnetic resonance imaging in human V1. *J. Neurosci.* **16:**4207–4221.

Büchel, C., Wise, R. J. S., Mummery, C. J., Poline, J. B., and Friston, K. J. 1996. Nonlinear regression in parametric activation studies. *Neuroimage* **4:**60–66.

Buxton, R., and Frank, L. 1997. A model for the coupling between cerebral blood flow and oxygen metabolism during neural stimulation. *J. Cereb. Blood Flow Metab.* **17:**64–72.

Cohen, M. S. 1996. Rapid MRI and functional applications. In *Brain Mapping: The Methods* (A. W. Toga and J. C. Mazziotta, Eds.), Academic Press, New York.

Cohen, M. S., Bookheimer, S. Y., and Mazziotta, J. C. 1995. Parametric analysis of functional MRI data: A physiologically relevant transform. In *Cerebral Blood Flow and Metabolism*.

Cohen, M. S., and Green, M. F. 1995. Where the voices come from: Imaging of schizophrenic auditory hallucinations. In *Society for Neuroscience*, Vol. 21, p. 259. San Diego, CA.

Cohen, M. S., Kelley, D. A., Rohan, M. L., and Roemer, P. A. 1996a. An MR instrument optimized for intracranial neuroimaging. In *Human Brain Mapping 96, Boston, MA*, pp. P1A1–007.

Cohen, M. S., Kosslyn, S. M., Breiter, H. C., DiGirolamo, G. J., Thompson, W. L., Bookheimer, S. Y., *et al.* 1996b. Changes in cortical activity during mental rotation: A mapping study using functional magnetic resonance imaging. *Brain* **119:** 89–100.

Cohen, M. S., and Weisskoff, R. M. 1991. Ultra-fast imaging. *Magn. Reson. Imaging* **9:**1–37.

Constable, R. T., Skudlarski, P., and Gore, J. C. 1995. An ROC approach for evaluating functional brain MR imaging and postprocessing protocols. *Magn. Reson. Med.* **34:**57– 64.

Dobkin, B. H., Cohen, M. S., Bookheimer, S. Y., and Mazziotta, J. C. 1996. Functional magnetic resonance imaging to study brain adaptations during rehabilitation of upper extremity function after hemiplegic stroke. *J. Neuro. Rehab.* **10:**136 [Abstract].

Engel, S. A., Rumelhart, D. E., Wandell, B. A., Lee, A. T., Glover, G. H., Chichilnisky, E. J., *et al.* 1994. fMRI of human visual cortex. *Nature* **369:**525. [Letter].

Farzaneh, F., Riederer, S. J., and Pelc, N. J. 1990. Analysis of T2 limitations and off-resonance effects on spatial resolution and artifacts in echo-planar imaging. *Magn. Reson. Med.* **14:**123– 139.

Fisel, C. R., Ackerman, J. L., Buxton, R. B., Garrido, L., Belliveau, J. W., Rosen, B. R., *et al.* 1991. MR contrast due to microscopically heterogeneous magnetic susceptibility: Numerical simulations and applications to cerebral physiology. *Magn. Reson. Med.* **17:**336–347.

Friston, K., Holmes, A., Poline, J., Grasby, P., Williams, S., Frackowiak, R., *et al.* 1995. Analysis of fMRI time series revisited. *Neuroimage* **2:** 45–53.

Friston, K., Jezzard, P., and Turner, R. 1994. Analysis of functional MRI time series. *Hum. Brain Mapping* **1:**153–171.

Friston, K. J., Dolan, R. J., and Frackowiak, R. S. J. 1991. *Statistical Parametric Mapping.* MRC Cyclotron Unit, Hammersmith Hospital, London, England.

Hong, X., Cohen, M., and Roemer, P. 1997. Functional EPI with real time imaging processing. In *Fifth Annual Meeting of the International Society for Magnetic Resonance in Medicine.* Vancouver, BC, pp. 321.

Jackson, G., Connelly, A., Cross, J., Gordon, I., and Gadian, D. 1994. Functional magnetic resonance imaging of focal seizures. *Neurology* **44:**850– 856.

Kwong, K. K., Belliveau, J. W., Chesler, D. A., Goldberg, I. E., Weisskoff, R. M., Poncelet, B. P., *et al.* 1992. Dynamic magnetic resonance imaging of human brain activity during primary sensory stimulation. *Proc. Natl. Acad. Sci. USA* **89:**5675– 5679.

Liu, C. L., and Liu, J. W. S. 1974. *Linear Systems Analysis.* McGraw-Hill, New York.

Malonek, D., and Grinvald, A. 1996. Interactions between electrical activity and cortical microcirculation revealed by imaging spectroscopy—Implications for functional brain mapping. *Science* **272:**551–554.

Mansfield, P. 1977. Multi-planar image formation using NMR spin echoes. *J. Phys. C* **10:**L55–L58.

Margosian, P. 1985. Faster MR imaging—Imaging with half the data. In *Society for Magnetic Resonance in Medicine,* p. 1024.

Mazziotta, J. C., and Phelps, M. E. 1984. Human sensory stimulation and deprivation: Positron emission tomographic results and strategies. *Ann. Neurol.* **15:**S50–S60.

Menon, R. S., Ogawa, S., Hu, X., Strupp, J. P., Anderson, P., and Ugurbil, K. 1995. BOLD based functional MRI at 4 Tesla includes a capillary bed contribution: Echo-planar imaging correlates with previous optical imaging using intrinsic signals. *Magn. Reson. Med.* **33:**453–459.

Ogawa, S., Tank, D. W., Menon, R., Ellermann, J. M., Kim, S. G., Merkle, H., *et al.* 1992. Intrinsic signal changes accompanying sensory stimulation: Functional brain mapping with magnetic resonance imaging. *Proc. Natl. Acad. Sci. USA* **89:**5951–5955.

Press, W., Vetterling, W., Teukolsky, S., and Flannery, B. 1992. *Numerical Recipes in C—The Art of Scientific Computing.* Cambridge Univ. Press, Cambridge.

Price, C., Wise, R., Ramsay, S., Friston, K., Howard, D., and Patterson, K., *et al.* 1992. Regional response differences within the human auditory cortex when listening to words. *Neurosci. Lett.* **146:**179–82.

Roy, C. S., and Sherrington, C. S. 1890. On the regulation of the blood-supply of the brain. *J. Physiol.* **11:** 85–108.

Savoy, R., O'Craven, K., Weisskoff, R., Davis, T., Baker, J., and Rosen, B. 1994. Exploring the temporal boundaries of fMRI: Measuring responses to very brief visual stimuli. In *Society for Neuroscience 24th Annual Meeting, Miama Beach, FL.* p. 518.4.

Schneider, W., Casey, B., and Noll, D. 1993. Functional MRI mapping of stimulus rate effects across visual processing stages. *Hum. Brain Mapping* **1:**117–133.

Schroeder, C. E., Steinschneider, M., Javitt, D. C., Tenke, C. E., Givre, S. J., Mehta, A. D., *et al.* 1995. Localization of ERP generators and identification of underlying neural. *Electroencephalogr. Clin. Neurophysiol. Suppl.* **44:**55–75.

Sereno, M. I., Dale, A. M., Reppas, J. B., Kwong, K. K., Belliveau, J. W., Brady, T. J., *et al.* 1995. Borders of multiple visual areas in humans revealed by functional magnetic resonance imaging. *Science* **268:** 889–893. [See comments].

Simpson, G. V., Pflieger, M. E., Foxe, J. J., Ahlfors, S. P., Vaughan, H. G., Jr., Hrabe, J., *et al.* 1995. Dynamic neuroimaging of brain function. *J. Clin. Neurophysiol.* **12:**432–449.

Tootell, R. B., Reppas, J. B., Kwong, K. K., Malach, R., Born, R. T., Brady, T. J., *et al.* 1995. Functional analysis of human MT and related visual cortical areas using magnetic resonance imaging. *J. Neurosci.* **15:**3215–3230.

Turner, R., Jezzard, P., Wen, H., Kwong, K. K., Le Bihan, D., Zeffiro, T., *et al.* 1993. Functional mapping of the human visual cortex at 4 and 1.5 tesla using deoxygenation contrast EPI. *Magn. Reson. Med.* **29:**277–279.

VanMeter, J., Maisog, J., Zeffiro, T., Hallett, M., Herscovitch, P., and Rapoport, S. 1995. Parametric analysis of functional neuroimages: Application to a variable-rate motor taks. *Neuroimage* **2:**273–283.

Warach, S., Levin, J. M., Schomer, D. L., Holman, B. L., and Edelman, R. R. 1994. Hyperperfusion of ictal seizure focus demonstrated by MR perfusion imaging. *AJNR Am. J. Neuroradiol.* **15:**965–968.

Weisskoff, R. M., Baker, J. R., Belliveau, J. W., Davis, T. L., Kwong, K. K., Cohen, M. S., *et al.* 1993. Power spectrum analysis of functionally-weighted MR data: What's in the noise? In *Society of Magnetic Resonance in Medicine,* p. 7. New York.

Worsley, K. J., Evans, A. C., Marrett, S., and Neelin, P. 1992. A three-dimensional statistical analysis for CBF activation studies in human brain. *J. Cereb. Blood Flow Metab.* **12:**900–918. [See comments]